inorganics

MDPI

Communication

Synthesis and Structural Comparisons of NHC-Alanes

Fáinché Murphy, Alan R. Kennedy and Catherine E. Weetman *

Department of Pure and Applied Chemistry, University of Strathclyde, 295 Cathedral Street, Glasgow G1 1XL, UK
* Correspondence: catherine.weetman@strath.ac.uk

Abstract: *N*-heterocyclic carbenes (NHCs) are widely used in organometallic chemistry. Here, we examine the role of NHCs in the stabilisation of aluminium hydrides, AlH_3, also known as alanes. This includes an assessment of the various synthetic strategies, comparisons of structural parameters and theoretical insight. Based on percent buried volume ($\%V_{bur}$) parameters, we report the largest and smallest NHC alanes to date, with noted differences in their observed stability in both the solution and solid state.

Keywords: *N*-heterocyclic carbenes; aluminium; main group

check for updates

Citation: Murphy, F.; Kennedy, A.R.; Weetman, C.E. Synthesis and Structural Comparisons of NHC-Alanes. *Inorganics* **2023**, *11*, 13. https://doi.org/10.3390/inorganics11010013

Academic Editors: Stephen Mansell and Simon Aldridge

Received: 5 December 2022
Revised: 16 December 2022
Accepted: 20 December 2022
Published: 26 December 2022

1. Introduction

N-heterocyclic carbenes (NHCs) play a vital role in modern day organometallic chemistry [1]. Their highly tuneable steric and electronic properties have made them a staple ligand choice for a variety of applications from transition metal catalysis to materials [2]. Within the chemistry of the main group elements, NHCs have been pivotal in the stabilisation of low-oxidation state species owing to their strong σ-donating and π-accepting nature [3]. The key role of NHCs in the stabilisation of reactive species has been particularly exemplified in the isolation of group 13 complexes [4]. In 1992, Arduengo and co-workers reported the synthesis and characterisation of $IMesAlH_3$ (**A**, IMes = 1,3-bis(2,4,6-trimethylphenyl)imidazoline-2-ylidene, Figure 1), which was reported to have a remarkable stability in the solid state (m.p. 246–247 °C) considering that there is a hydride next to a electrophilic donor [5]. Other notable examples of the importance of NHCs in group 13 chemistry are the stabilisation of group 13 multiply bonded species with the first example of a boron-boron triple bond (**B**) [6] and a neutral aluminium–aluminium double bond (**C**) (Figure 1) [7,8].

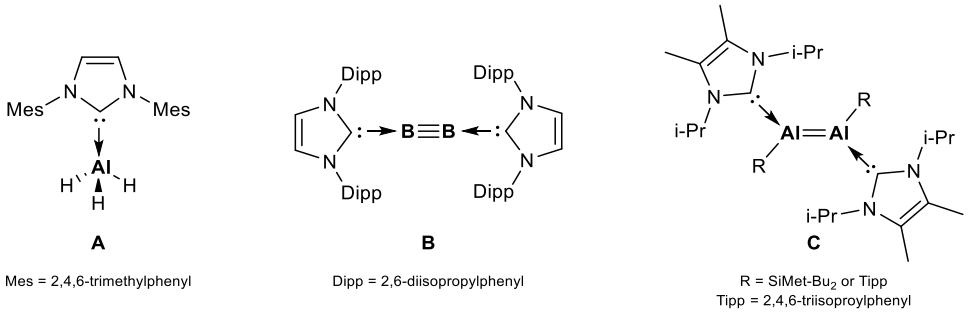

Figure 1. Examples of NHC-stabilised group 13 complexes.

In regard to NHC-stabilised group 13 complexes, those involving aluminium are the least well-studied to date, which is surprising given its high natural abundance and low cost, making aluminium a desirable metal to work with. In addition, the high stability and Lewis acidity of Al(III) trialkyl and trihalide derivatives have led to them being widely used in Zieglar-Natta and Friedel-Crafts reactions, respectively [9,10]. Furthermore, recent studies have shown the developing role of ligated aluminium-hydrides in hydroelementation

and dehydrocoupling catalysis [11–17], as well as the use of commercially available Al-H containing species such as $LiAlH_4$ and DIBAL-H for hydrogenation and hydroboration catalysis [18–20].

In terms of trivalent NHC-aluminium compounds, they have been used for a variety of studies which includes the exploration of the coordination chemistry of NHC-alanes towards 14- and 16-electron transition metal complexes [21,22] as well as ring expansion and ring opening reactions of NHCs [23,24]. Also of note, is the formation of abnormal NHCs (aNHC) in reactions with aluminium reagents. Dagorne and co-workers reported that ItBu (ItBu = 1,3-di-*tert*-butylimidazoline-2-ylidene) isomerises to the abnormal position, on reaction with $AlMe_3$, due to the steric congestion around the aluminium centre [25,26]. Furthermore, it was shown that using the sterically demanding $Al(iBu_2)TMP$ (TMP = 2,2,6,6-tetramethylpiperidine) reagent with ItBu results in direct formation of the abnormal NHC (aNHC) complex [27]. Additionally, in the case of $ItBuAlH_3$ it has been shown that abnormal formation can be promoted through use of polar solvents [28]. Whilst these examples show the effect of increasing the steric congestion at the aluminium centre, as well as importance of the reaction solvent, we were interested in assessing the steric demands of the NHC ligand itself, and its subsequent influence on the stability of the corresponding aluminium complexes in the solution and solid state.

Figure 2 shows NHCalanes (**A**, **D**–**G**) [5,28–31] that are reported in the Cambridge structural database (CSD), arranged in order of increasing percent buried volume ($\%V_{bur}$) [32,33]. It is important to note that examples of ring-expanded NHCs or substituted backbones [4] are also reported but to directly compare the influence of the 'wing-tip' substituents we focused on the simple unsaturated backbone. With this in mind, we were interested in adding to the small number of NHC-alanes that have been structurally characterised and assessing the influence of varying the steric and electronic properties on stability of these complexes. As such, we focused on adding to either end of the $\%V_{bur}$ scale. Firstly, IPr* ($\%V_{bur}$ = 42.6, IPr* = 1,3-bis(2,6-bis(diphenylmethyl)-4-methylphenyl)imidazol-2-ylidene) is a bulky-yet-flexible NHC ligand that has shown promise in a variety of transition metal catalysis [34]; secondly, ICy ($\%V_{bur}$ = 26.4, ICy = 1,3-bis(cyclohexyl)imidazol-2-ylidene) has been used in transition metal chemistry but there is only one structurally characterised example with a main group element [35].

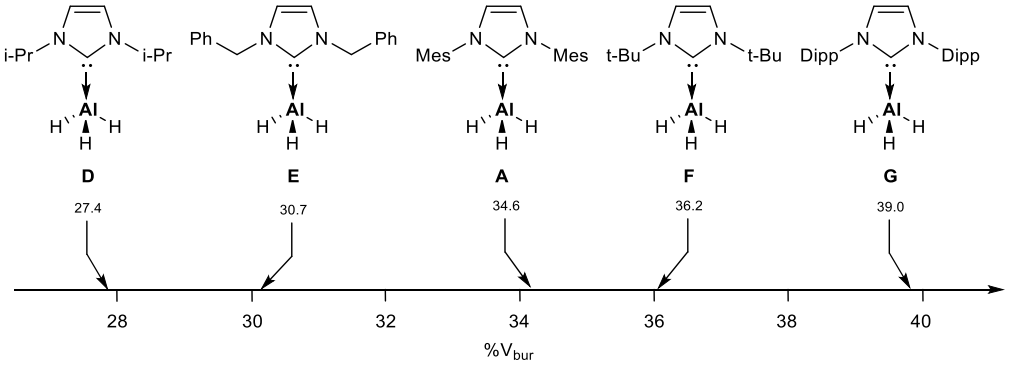

Figure 2. Reported NHC-alanes [5,28–31] vs. percent buried volume ($\%V_{bur}$).

2. Results and Discussion

2.1. Assessment of NHC-Alane Synthetic Routes

As an entry point into this chemistry, we initially re-examined the synthetic routes required to make NHC-alanes. Given the literature precedent, we opted to use $IDippAlH_3$ as the benchmark for determining the most efficient synthetic route taking into consideration ease of synthesis, by-product formation and atom efficiency. As can be seen in Scheme 1, there are three main routes that can be used: route A via the free carbene, route B by direct formation, and route C via transmetallation.

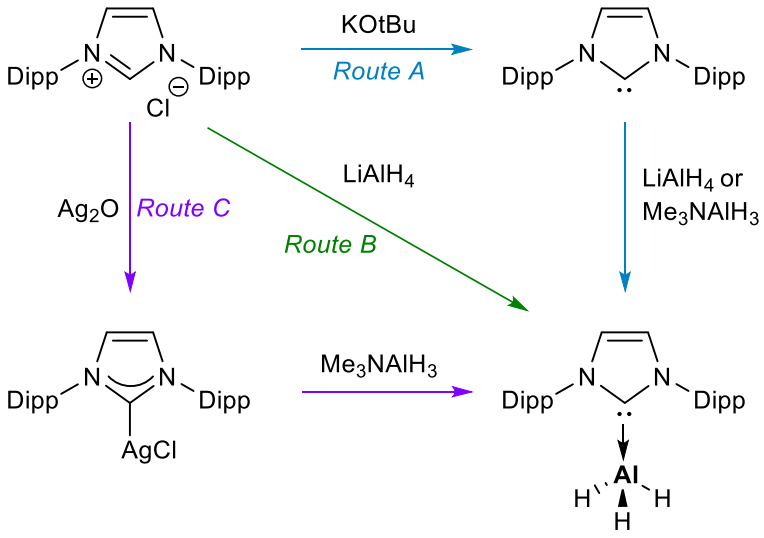

Scheme 1. Synthetic routes to access NHC-alanes.

Following route A, the literature reports excellent yields for the deprotonation step (80–95%) with clean conversion to IDipp, and minimal by-products, which can easily be removed through celite filtration [36]. The second step of this reaction can proceed either with commercially available $LiAlH_4$ or with Me_3NAlH_3. The literature reports yields of 75% for the reaction with $LiAlH_4$, following removal of LiH by-products [31]. In addition, we observed the formation of the corresponding imidazolidine ($IDippH_2$) during this reaction, further decreasing yields. In contrast, whilst Me_3NAlH_3 is required to be synthesised in advance, clean adduct formation was observed in near quantitative yields (90–95%). Thus, the use of Me_3NAlH_3 was preferred over the use of $LiAlH_4$ due to the production of gaseous NMe_3 instead of solid LiH as a by-product, resulting in a much simpler work-up.

Route B provides the least number of experimental steps, and on paper, provides the most economical approach to synthesise NHC-stabilised alanes. However, the addition of $LiAlH_4$ to IDipp.HCl resulted in the clean formation of the undesirable imidazolidine, as characterised by ^{1}H NMR. In the ^{1}H NMR spectrum, loss of the downfield imidazolium proton signal was observed, with a new singlet (corresponding to two protons) residing at 5.64 ppm for $IDippH_2$. Similar outcomes were observed in the use of Me_3NAlH_3 with IDipp.HCl, thus route B is not recommended.

Finally, route C via transmetallation was investigated. This offers the advantage that the formation of the silver carbene complex can be carried out under air adding to the ease of synthesis and isolation. With IDippAgCl in hand transmetallation was trialled with Me_3NAlH_3; this did result in the desired product formation but in decreased yields of 45%. It is of note, that a recent study by Timoshkin and Balova for the formation of $NHCAlCl_3$ compounds highlighted that copper is a better carbene transfer agent than silver for strong Lewis acidic metals [37]. However, given the low-atom efficiency we chose not to pursue this route further.

To summarise, route A via free carbene and adduct formation with Me_3NAlH_3 provides the best strategy to access NHC-alanes due to high yielding steps with minimal by-product formation.

2.2. Synthesis of NHC-Alanes

2.2.1. Synthesis and Characterisation of IPr*AlH_3 (**1**)

The recent development of a new generation of bulky yet flexible NHCs by Bertrand [38] and Markó [39] has provided access to a new range of complexes and reactivity due to the advantageous ligand flexibility towards incoming substrates. In 2009, Markó and co-workers reported the synthesis of IPr*: an easily accessible, highly hindered NHC [39]. Essentially a bulkier version of the popular IDipp, the synthesis of IPr* was achieved by

the replacement of methyl groups of IDipp with phenyl rings. Due to the "flexible steric bulk" and ease of synthesis we were interested to study the stabilisation effects of IPr* with alanes and whether this much larger NHC ligand would result in normal or abnormal carbene formation.

Following successful deprotonation of the IPr*.HX salt (X = Cl or BF4) [40], a 1:1.1 reaction of IPr* with Me_3NAlH_3 in diethyl ether, at room temperature afforded the desired alane complex, IPr*AlH_3 (**1**) in high yields of 88 % (Scheme 2).

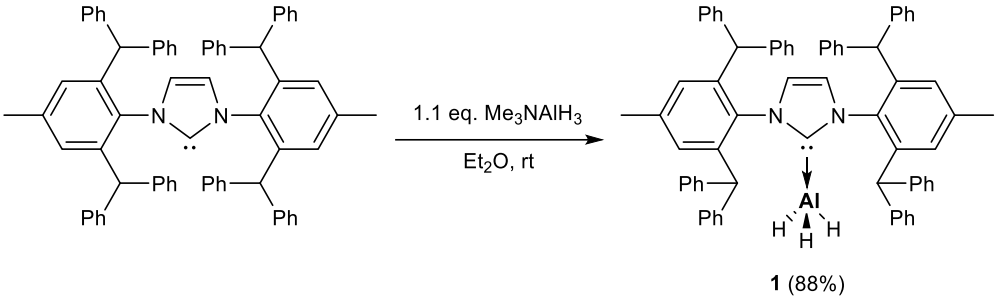

Scheme 2. Synthesis of IPr*AlH_3 (**1**).

The formation of compound **1** was confirmed on inspection of the ^{1}H NMR spectrum. A new broad resonance for the hydride ligands were observed at 4.36 ppm, as well as a shift in the characteristic signals (C*H*$(Ph)_2$ and NHC backbone) associated with the IPr* ligand. The C*H*$(Ph)_2$ signal (accounting for four protons) shifted upfield from 6.03 ppm to 5.68 ppm, and the C*H* signals for the NHC backbone (accounting for two protons) shifted upfield from 5.79 ppm to 5.32 ppm upon coordination to alane. Further confirmation that the NHC ligand was indeed coordinated to the alane was observed in the $^{13}C\{^1H\}$ NMR spectrum, where the NCN signal was found at 176.8 ppm, indicating coordination as the free carbene carbon of IPr* is around 220 ppm. No signal was observed in the $^{27}Al\{^1H\}$ NMR spectrum, similar to other NHC-alanes.

The infrared spectrum of IPr*AlH_3 shows a broad stretch at 1760 cm^{-1} confirming the presence of an AlH_3 unit. This is in the same region as other reported NHC-alane adducts (e.g., IDippAlH_3 ν(Al-H) 1729 cm^{-1}) [31]. One of the notable features of the original IMesAlH_3 (compound **A**) was the reported high thermal stability (m.p. 246–247 °C) [5], and compound **1** was found to exhibit similar properties in the solid state (m.p. 230 °C). However, whilst compound **1** has a high thermal stability care must be taken when drying the compound under vacuum (either for prolonged periods or use of a warm water bath) as the alane fragment sublimes into the solvent trap, resulting in the isolation of the free carbene.

In the solution state the onset of decomposition was observed at 60 °C, with full decomposition after 16 h. A major decomposition product was identified as IPr*H_2 with several other unidentified minor species observed in the ^{1}H NMR spectrum. It is possible that normal to abnormal rearrangement may have occurred along with a variety of ring opening or ring-expansion reactions in line with previous studies [23].

Crystals suitable for single crystal X-ray crystallography (SC-XRD) were grown via hexane diffusion into a toluene solution at −25 °C. The solid-state structure is shown in Figure 3 and is consistent with spectroscopic data. The steric protection afforded by the extremely bulky NHC is evident from its solid-state structure; the two aromatic substituents are close to perpendicular with the imidazole ring and the diphenyl methyl groups are folded back from the aluminium centre. The hydride ligands were refined isotropically with an average bond length of 1.54 Å which is similar to the mean value (1.53 Å) for previously determined terminal Al-H bonds. The Al-C bond length of 2.070(2) Å is slightly longer than those reported for aryl containing NHCAlH_3 species (**G**, IDippAlH_3 (2.056(1) Å) and **A**, IMesAlH_3 (2.034(3) Å), but similar to the sterically demanding ItBuAlH_3, **F**, (2.083(11) Å).

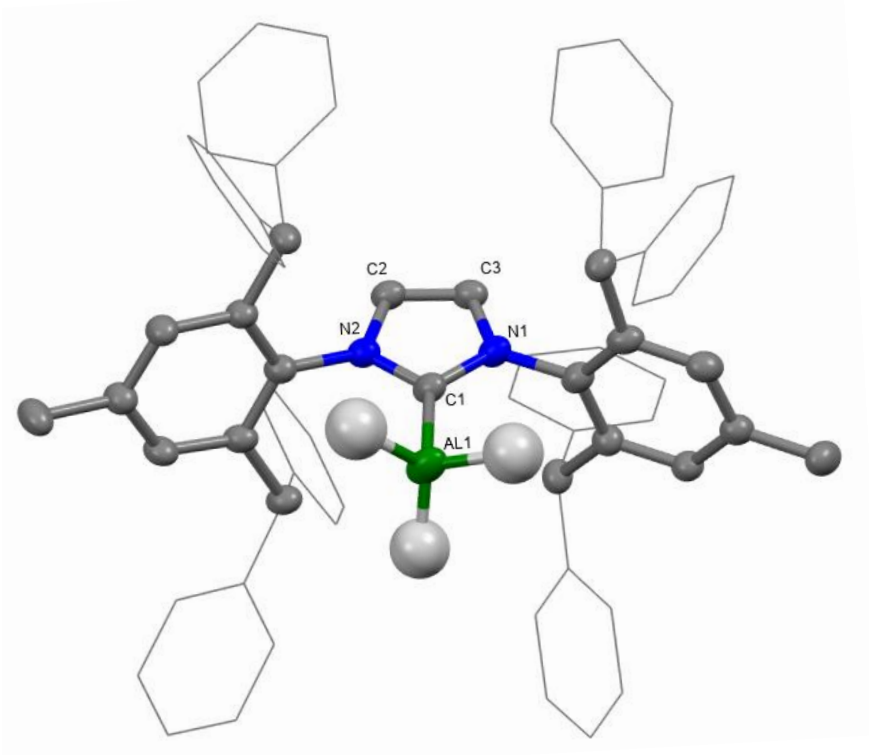

Figure 3. Solid-state structure of IPr*AlH_3 (**1**) with ellipsoids drawn at 50% probability, peripheral phenyl rings have been depicted in wireframe for clarity. Solvent and hydrogen atoms other than those on aluminium have been omitted for clarity. Selected bond lengths (Å) and angles (°): Al(1)–C(1) 2.070(2), C(1)–N(1) 1.357(3) C(1)–N(2) 1.369(3), C(2)–C(3) 1.342(3), Average Al-H 1.54, N(1)–C(1)-N(2) 104.09(18).

2.2.2. Synthesis and Characterisation of ICyAlH$_3$ (**2**)

Following the standard procedure, a 1:1.1 reaction of ICy with Me_3NAlH_3 in toluene afforded the alane complex, ICyAlH$_3$ in a good yield of 81% (Scheme 3).

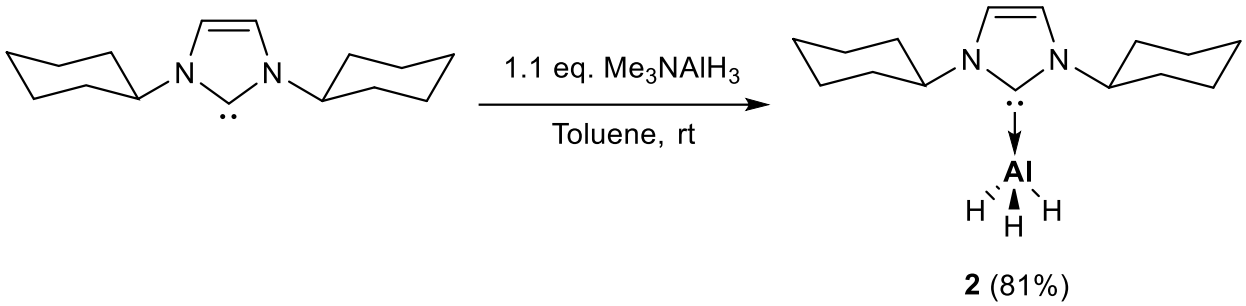

Scheme 3. Synthesis of ICyAlH$_3$ (**2**).

Similar to compound **1**, ICyAlH$_3$ formation was confirmed upon inspection of the NMR spectra. Key signals for the NHC backbone were noted to have shifted from 6.62 ppm to 6.52 ppm compared to the starting material. More definitively, a broad signal was observed at 4.62 ppm indicating that a Al-*H* species is present as well as a corresponding signal observed in the $^{27}Al\{^1H\}$ NMR spectrum at 108 ppm which is line with those previously reported (**A** 107 ppm [5] and **D** 106 ppm [29]). Further confirmation is gained from the $^{13}C\{^1H\}$ NMR spectra wherein the carbene signal has shifted from 212.3 ppm (ICy) to 170.1 ppm on coordination of the alane. Compound **2** was found to exhibit decreased thermal stability in the solid state (136 °C) as well as in the solution state. Here we found that decomposition to ICyH$_2$ began to occur at ca. 30–40 °C. Care must therefore be taken

when removing the toluene solution, as the use of a warm bath promotes formation of $ICyH_2$. The synthesis is also possible in Et_2O for ease of work-up, but results in a decreased overall yield (*ca.* 60%).

SC-XRD quality crystals were obtained from a concentrated toluene solution at −25 °C and the solid-state structure is shown in Figure 4. Similar to compound **1**, the two cyclohexyl substituents are close to perpendicular to the imidazole ring. The Al-C bond length of 2.055(11) Å is comparable to previously reported NHC-alanes (**A**, **D**–**G**) [5,28–31].

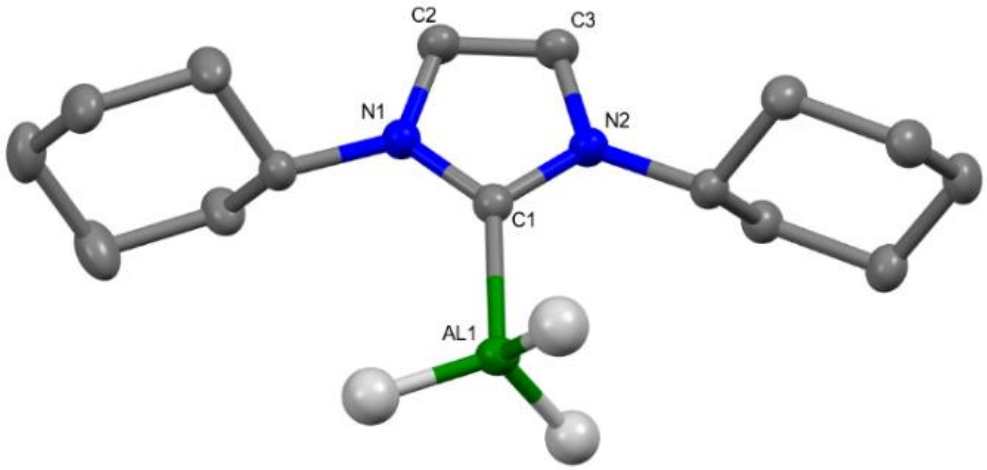

Figure 4. Solid-state structure of $ICyAlH_3$ (**2**) with ellipsoids drawn at 50 % probability. Hydrogen atoms other than those on aluminium have been omitted for clarity. Selected bond lengths (Å) and angles (°): Al(1)–C(1) 2.055(11), C(1)–N(1) 1.3544(14), C(1)–N(2) 1.3835(14), C(2)–C(3) 1.3512(16), Average Al-H 1.527, N(1)–C(1)–N(2) 104.83(9).

2.3. Steric and Electronic Properties of NHC-Alanes

As mentioned in the introduction, we are interested in the steric and electronic effects of NHC ligands on the stability of NHC-alanes. To investigate this, we compared several different experimental parameters as shown in Table S1 in the supporting information. Experimentally, the only item of note is that compound **2** is much less thermally stable compared to aryl NHC-alanes by approximately 100 °C. However, given the lack of data for other alkyl NHC-alanes in the literature it is unclear if this is a general observation.

As such we turned to theory to gain further insight. Geometry optimisations and Natural Bond Orbital (NBO) analysis of $ICyAlH_3$ (**2**) and $IPhAlH_3$ were performed at the M06-2X/6–311+G(d,p) level of theory using Gaussian 16 and 09, respectively (see supporting information for full details). These two NHC-alanes were chosen to directly compare the influence of alkyl vs. aryl congeners, whilst no experimental data exist for IPh this was chosen in the interest of computational simplicity over substituted aryl groups. In general, good agreement was found between experimental and calculated structural parameters (see supporting information), with similar HOMO-LUMO gaps also calculated ($ICyAlH_3$ 7.72 eV vs. $IPhAlH_3$ 7.23 eV). Wiberg Bond Indices (WBI) for the Al-C_{NHC} bonds also are similar ($ICyAlH_3$ 0.52 vs. $IPhAlH_3$ 0.50). NBO analysis (Figure 5) indicates a highly polarised Al-C_{NHC} σ-bond in the case of $ICyAlH_3$ (Al 16%, C 84%), whereas, the Al-C_{NHC} bond in $IPhAlH_3$ indicates more dative character with donation of the carbene carbon lone pair into the empty Al *p*-orbital (Second order perturbation theory (SOPT) LP C7>LV Al 149 kcal mol^{-1}), as one may expect based on Lewis structural representation. Caution is taken here as to not over-analyse these findings, but differences here are in line with the electron donating character of alkyl groups vs. the electron withdrawing nature of aryl groups.

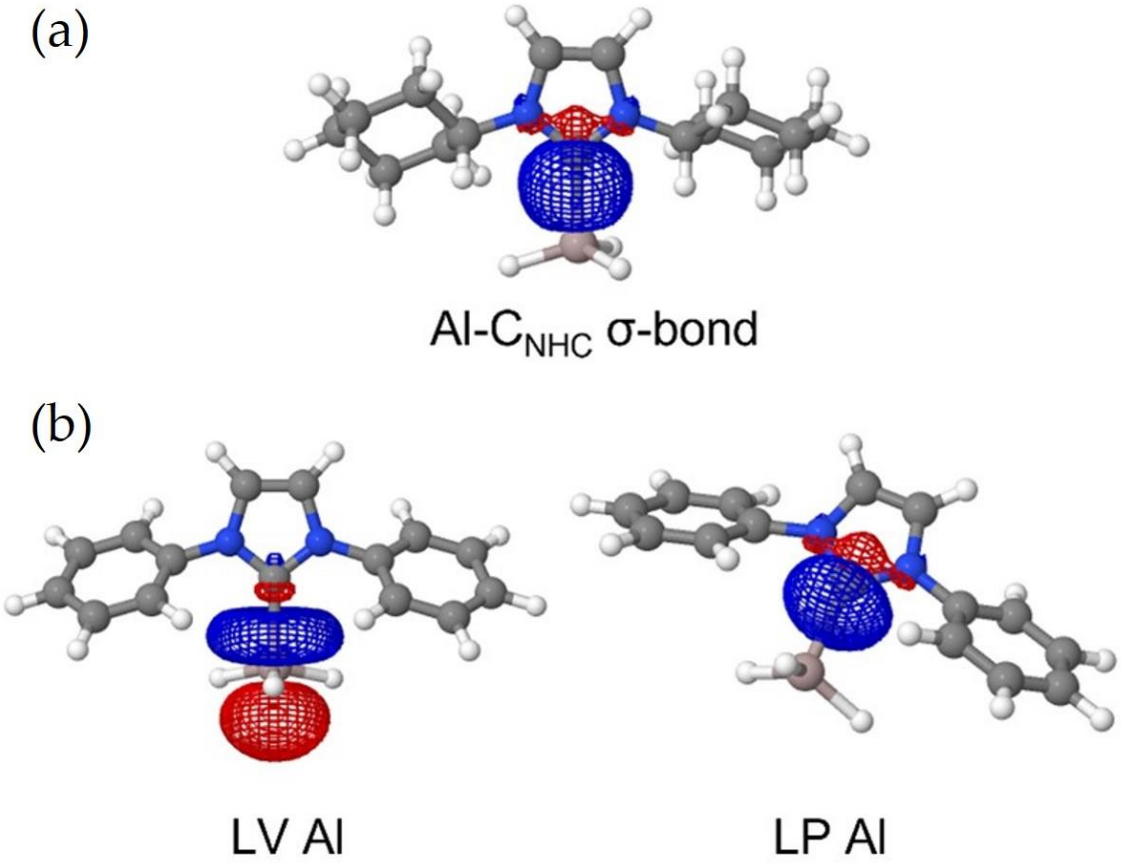

Figure 5. NBO visualisations for (**a**) $ICyAlH_3$ and (**b**) $IPhAlH_3$. LV = lone valency, LP = lone pair.

3. Conclusions

In summary, we have assessed the various routes used for the synthesis of NHC-alanes and used the optimised method via free carbenes to isolate two new NHC-alane complexes. Compounds **1** and **2** are currently the largest and smallest reported NHCs based on $\%V_{bur}$, respectively. Examination of various experimental parameters as well as steric and electronic properties revealed no clear correlation of the observed stability of NHC-alanes.

4. Materials and Methods

4.1. General Methods and Instruments

All air- and moisture-sensitive synthetic work was carried out under an inert gas atmosphere (N_2 or Ar) using a glovebox and/or vacuum line using standard Schlenk techniques. Celite and 4Å molecular sieves were dried in an oven overnight at 150 °C prior to use. All glassware was heated under vacuum using a heat gun prior to use. For air- and moisture-sensitive reactions, toluene was provided by an Innovative Technology Solvent Purification System. THF, hexane and diethyl ether were dried by distillation over sodium benzophenone ketyl prior to use. All solvents were stored under nitrogen over molecular sieves activated at 150 °C in vacuo. C_6D_6 was purchased from Fluorochem, taken into a glovebox and stored over activated 4 Å molecular sieves under argon.

All reagents were purchased from Sigma-Aldrich, Fluorochem or Alfa Aesar and used as purchased.

Air- and moisture-sensitive NMR experiments were conducted in a J-Young NMR tube and were made and sealed in a glovebox. All other air- and moisture-sensitive samples were prepared using regular NMR tubes and caps secured with parafilm in a glovebox. Air stable NMR samples were prepared open to air and moisture using regular NMR tubes and

caps. All spectra were recorded on a Bruker AV3-400 spectrometer equipped with a liquid nitrogen Prodigy cryoprobe operating at 400.4 MHz (^{1}H), 100.7 MHz (^{13}C), 104.3 MHz (^{27}Al), and were measured at 300 K. All chemical shifts are expressed in parts per million (δ, ppm). ^{1}H NMR chemical shifts are referenced to residual proton resonances of the corresponding deuterated solvent C_6D_5H (δ = 7.16 ppm, C_6D_6) and $CHCl_3$ (δ = 7.26 ppm, $CDCl_3$. ^{13}C NMR chemical shifts are reported relative to TMS using the carbon resonances of the deuterated solvent C_6D_6 (δ = 128.06 ppm), $CDCl_3$ (δ = 77.16 ppm). All ^{13}C and ^{27}Al NMR spectra were obtained with ^{1}H broadband decoupling.

Infrared spectra were performed on a Bruker Tensor 27 spectrometer with a MKII Reflection Golden Gate Single Diamond ATR system. The position of the absorption bands is given in wavenumbers [cm^{-1}].

Crystallographic data for compounds **1** and **2** were measured with a Rigaku Synergy-i instrument with monochromated Cu−Kα (λ 1.54184 Å) radiation. The measured data was processed with the CrysAlisPro [41] software package. The structures were solved with the ShelXT [42] structure solution program and refined with ShelXL-2018 [2] to convergence against F^2. Final refinement was within WinGX [43].

All quantum chemical calculations were carried out using the Gaussian16 package [44]. The NBO analyses [45] were performed with version 6.0 [46] which was implemented in the G09 D.01 version of the Gaussian program [47]. The molecular structure optimizations were performed using the M06-2X [48] functional along with the 6-311+G(d,p) basis set. For the visualization of the natural bond orbitals the program Jmol was used [49].

*4.2. Synthesis of IPr*AlH$_3$ (**1**)*

In a glovebox, IPr* (150 mg, 0.165 mmol, 1.0 equiv.) and Me_3NAlH_3 (20 mg, 0.181 mmol, 1.1 equiv.) were combined in a Schlenk flask. On the Schlenk line, the solids were suspended in dry diethyl ether (12 mL) and the reaction mixture was stirred at room temperature overnight. The white suspension was slowly concentrated to dryness under reduced pressure to give a white solid. Yield: 135 mg, 88%. SC-XRD quality crystals were produced through hexane diffusion into a concentrated toluene solution at -25 °C. ^{1}H NMR (400 MHz, C_6D_6) δ_H (ppm): 7.66 (d, J = 7.5 Hz, 8H, H_{Ar}), 7.20–6.86 (m, 36H, H_{Ar}), 5.68 (s, 4H, C*H*Ph$_2$), 5.32 (s, 2H, NC*H*C*H*N), 4.36 (bs, Al-*H*), 1.69 (s, 6H, C*H*$_3$). ^{13}C{^{1}H} NMR (100 MHz, C_6D_6) δ_C (ppm): 176.8 (C_{Ar}), 144.3 (C_{Ar}), 143.6 (C_{Ar}), 142.0 (C_{Ar}), 140.6 (C_{Ar}), 134.4 (C_{Ar}), 130.9 (C_{Ar}), 130.5 (C_{Ar}), 129.9 (C_{Ar}), 128.8 (C_{Ar}), 128.5 (C_{Ar}), 127.2 (C_{Ar}), 126.8 (C_{Ar}), 124.2 (NCHCHN), 52.0 ($CHPh_2$), 21.3 (CH_3). IR (cm^{-1}): 1735 (Al-H).

*4.3. Synthesis of ICyAlH$_3$ (**2**)*

In a glovebox, ICy (100 mg, 0.430 mmol, 1 equiv.) and Me_3NAlH_3 (42 mg, 0.237 mmol, 1.1 equiv.) were combined in a vial and suspended in toluene (2 mL). The reaction mixture was left to stir for 4 h. Solvent was removed under reduced pressure to produce a yellow solid. Solid was re-dissolved in minimal toluene, filtered and placed in the −25 °C freezer. Crystalline material was produced after 1 week. Residual solvent was removed via pipette and the yellow solid was washed with benzene and dried under reduced pressure. Yield: 102 mg, 81%. SC-XRD quality crystals were produced from a concentrated toluene solution at −25 °C. ^{1}H NMR (400 MHz, C_6D_6) δ_H (ppm): 6.47 (s, 2H, NC*H*C*H*N), 4.93 (tt, $^{1}J_{HH}$ = 11.7 Hz, $^{2}J_{HH}$ = 3.8 Hz, 2H, C*H*), 4.51 (bs, Al-*H*), 1.91–0.81 (m, 20H, CH_2). ^{13}C{^{1}H} NMR (100 MHz, C_6D_6) δ_C (ppm): 170.1 (NCN), 117.7 (*C*H), 59.0 (*C*H), 34.1 (CH_2), 25.4 (CH_2), 25.3 (CH_2). ^{27}Al{^{1}H} NMR (104.3 MHz, C_6D_6) δ_{Al} (ppm): 108.3, ω1/2 (ppm): 15.3. IR (cm^{-1}): 1723, 1785.

Supplementary Materials: The following supporting information can be downloaded at: https://www.mdpi.com/article/10.3390/inorganics11010013/s1, Figures S1–S4: NMR spectra; Figures S5 and S6: NBO visualisation; Table S1: comparisons of NHCAlanes, Table S2: Selected Crystallographic and Refinement Parameters, Tables S3–S11: Computational Data.

Author Contributions: Conceptualisation, C.E.W.; methodology, C.E.W.; formal analysis, A.R.K.; investigation, F.M.; resources, F.M.; writing—original draft preparation, C.E.W. and F.M.; writing—review and editing, C.E.W., F.M and A.R.K.; visualisation, C.E.W.; supervision, C.E.W.; project administration, C.E.W.; funding acquisition, C.E.W. All authors have read and agreed to the published version of the manuscript.

Funding: This research received no external funding.

Institutional Review Board Statement: Not applicable.

Informed Consent Statement: Not applicable.

Data Availability Statement: X-ray crystallography data can be found through the CCDC (2221316 and 2221317, **1** and **2**, respectively). All other data can be found in the Supplementary Materials.

Acknowledgments: We thank David Nelson for the initial gift of NHC salts, as well as insightful discussions. We also thank Lena Albers and the Mulvey/O'Hara/Robertson groups for many insightful and entertaining discussions. Results were obtained using the ARCHIE-WeSt High Performance Computer (www.archie-west.ac.uk) based at the University of Strathclyde (Grant code EP/K000586/1). C.E.W. would like to thank the University of Strathclyde for the award of a Chancellor's Fellowship and the award of a student (F.M).

Conflicts of Interest: The authors declare no conflict of interest.

References

1. Nolan, S.P. *N-Heterocyclic Carbenes: Effective Tools for Organometallic Synthesis*; Wiley: Weinheim, Germany, 2014.
2. Bellotti, P.; Koy, M.; Hopkinson, M.N.; Glorius, F. Recent advances in the chemistry and applications of N-heterocyclic carbenes. *Nat. Rev. Chem.* **2021**, *5*, 711–725. [CrossRef]
3. Nesterov, V.; Reiter, D.; Bag, P.; Frisch, P.; Holzner, R.; Porzelt, A.; Inoue, S. NHCs in Main Group Chemistry. *Chem. Rev.* **2018**, *118*, 9678–9842.
4. Fliedel, C.; Schnee, G.; Aviles, T.; Dagorne, S. Group 13 metal (Al, Ga, In, Tl) complexes supported by heteroatom-bonded carbene ligands. *Coord. Chem. Rev.* **2014**, *275*, 63–86. [CrossRef]
5. Arduengo, A.J., III; Dias, H.R.; Calabrese, J.C.; Davidson, F. A stable carbene-alane adduct. *J. Am. Chem. Soc.* **1992**, *114*, 9724–9725. [CrossRef]
6. Braunschweig, H.; Dewhurst, R.D.; Hammond, K.; Mies, J.; Radacki, K.; Vargas, A. Ambient-temperature isolation of a compound with a boron-boron triple bond. *Science* **2012**, *336*, 1420–1422. [CrossRef] [PubMed]
7. Bag, P.; Porzelt, A.; Altmann, P.J.; Inoue, S. A stable neutral compound with an aluminum–aluminum double bond. *J. Am. Chem. Soc.* **2017**, *139*, 14384–14387. [CrossRef]
8. Weetman, C.; Porzelt, A.; Bag, P.; Hanusch, F.; Inoue, S. Dialumenes—Aryl vs. silyl stabilisation for small molecule activation and catalysis. *Chem. Sci.* **2020**, *11*, 4817–4827. [CrossRef]
9. Boor, J.; Boor, J. *Ziegler-Natta Catalysts and Polymerisations*; Academic Press: New York, NY, USA, 1979.
10. Olah, G.A. *Friedel-Crafts and Related Reactions*; John Wiley & Sons: New York, NY, USA, 1963.
11. Yang, Z.; Zhong, M.; Ma, X.; De, S.; Anusha, C.; Parameswaran, P.; Roesky, H.W. An Aluminum Hydride That Functions like a Transition-Metal Catalyst. *Angew. Int. Ed. Chem.* **2015**, *54*, 10225–10229. [CrossRef] [PubMed]
12. Jakhar, V.K.; Barman, M.K.; Nembenna, S. Aluminum monohydride catalyzed selective hydroboration of carbonyl compounds. *Org. Lett.* **2016**, *18*, 4710–4713. [CrossRef]
13. Jin, D.; Ma, X.; Liu, Y.; Peng, J.; Yang, Z. Novel aluminium compounds derived from Schiff bases: Synthesis, characterization and catalytic performance in hydroboration. *Appl. Organomet. Chem.* **2019**, *33*, e4637. [CrossRef]
14. Zhang, G.; Wu, J.; Zeng, H.; Neary, M.C.; Devany, M.; Zheng, S.; Dub, P.A. Dearomatization and Functionalization of Terpyridine Ligands Leading to Unprecedented Zwitterionic Meisenheimer Aluminum Complexes and Their Use in Catalytic Hydroboration. *ACS Catal.* **2019**, *9*, 874–884. [CrossRef]
15. Pollard, V.A.; Fuentes, M.Á.; Kennedy, A.R.; McLellan, R.; Mulvey, R.E. Comparing neutral (monometallic) and anionic (bimetallic) aluminum complexes in hydroboration catalysis: Influences of lithium cooperation and ligand set. *Angew. Int. Ed. Chem.* **2018**, *57*, 10651–10655. [CrossRef]
16. Franz, D.; Sirtl, L.; Pöthig, A.; Inoue, S. Aluminum Hydrides Stabilized by N-Heterocyclic Imines as Catalysts for Hydroborations with Pinacolborane. *Anorg. Allg. Chem.* **2016**, *642*, 1245–1250. [CrossRef]
17. Weetman, C.; Ito, N.; Unno, M.; Hanusch, F.; Inoue, S. NHI-and NHC-supported Al (III) hydrides for amine–borane dehydrocoupling catalysis. *Inorganics* **2019**, *7*, 92. [CrossRef]
18. Bismuto, A.; Cowley, M.J.; Thomas, S.P. Aluminum-catalyzed hydroboration of alkenes. *ACS Catal.* **2018**, *8*, 2001–2005. [CrossRef]
19. Bismuto, A.; Thomas, S.P.; Cowley, M.J. Aluminum Hydride Catalyzed Hydroboration of Alkynes. *Angew. Int. Ed. Chem.* **2016**, *55*, 15356–15359. [CrossRef]

20. Elsen, H.; Färber, C.; Ballmann, G.; Harder, S. $LiAlH_4$: From Stoichiometric Reduction to Imine Hydrogenation Catalysis. *Angew. Int. Ed. Chem.* **2018**, *57*, 7156–7160. [CrossRef]
21. Abdalla, J.A.; Riddlestone, I.M.; Tirfoin, R.; Phillips, N.; Bates, J.I.; Aldridge, S. Al–H σ-bond coordination: Expanded ring carbene adducts of AlH_3 as neutral bi-and tri-functional donor ligands. *Chem. Commun.* **2013**, *49*, 5547–5549. [CrossRef]
22. Riddlestone, I.M.; Edmonds, S.; Kaufman, P.A.; Urbano, J.; Bates, J.I.; Kelly, M.J.; Thompson, A.L.; Taylor, R.; Aldridge, S. σ-Alane complexes of chromium, tungsten, and manganese. *J. Am. Chem. Soc.* **2012**, *134*, 2551–2554. [CrossRef]
23. Schneider, H.; Hock, A.; Bertermann, R.; Radius, U. Reactivity of NHC Alane Adducts towards N-Heterocyclic Carbenes and Cyclic (Alkyl)(amino) carbenes: Ring Expansion, Ring Opening, and Al−H Bond Activation. *Chem. Eur. J.* **2017**, *23*, 12387–12398. [CrossRef]
24. Anker, M.D.; Colebatch, A.L.; Iversen, K.J.; Wilson, D.J.; Dutton, J.L.; Garcia, L.; Hill, M.S.; Liptrot, D.J.; Mahon, M.F. Alane-Centered Ring Expansion of N-Heterocyclic Carbenes. *Organometallics* **2017**, *36*, 1173–1178. [CrossRef]
25. Schmitt, A.L.; Schnee, G.; Welter, R.; Dagorne, S. Unusual reactivity in organoaluminium and NHC chemistry: Deprotonation of $AlMe_3$ by an NHC moiety involving the formation of a sterically bulky NHC–$AlMe_3$ Lewis adduct. *Chem. Commun.* **2010**, *46*, 2480–2482. [CrossRef] [PubMed]
26. Schnee, G.; Nieto Faza, O.; Specklin, D.; Jacques, B.; Karmazin, L.; Welter, R.; Silva López, C.; Dagorne, S. Normal-to-Abnormal NHC Rearrangement of AlIII, GaIII, and InIII Trialkyl Complexes: Scope, Mechanism, Reactivity Studies, and H_2 Activation. *Chem. Eur. J.* **2015**, *21*, 17959–17972. [CrossRef] [PubMed]
27. Pollard, V.A.; Fuentes, M.A.; Robertson, S.D.; Weetman, C.; Kennedy, A.R.; Brownlie, J.; Angus, F.J.; Smylie, C.; Mulvey, R.E. Reactivity studies and structural outcomes of a bulky dialkylaluminium amide in the presence of the N-heterocyclic carbene, ItBu. *Polyhedron* **2021**, *209*, 115469. [CrossRef]
28. Chernysheva, A.M.; Weinhart, M.; Scheer, M.; Timoshkin, A.Y. Normal to abnormal ItBu·AlH_3 isomerization in solution and in the solid state. *Dalton. Trans.* **2020**, *49*, 4665–4668. [CrossRef]
29. Francis, M.; Hibbs, D.; Hursthouse, M.; Smithies, N. Carbene complexes of Group 13 trihydrides: Synthesis and characterisation of [MH_3 {CN (Pr^i) C_2Me_2N (Pr^i)}], M = Al, Ga or In. *J. Chem. Soc. Dalton Trans.* **1998**, *19*, 2349–2354. [CrossRef]
30. Cao, L.L.; Daley, E.; Johnstone, T.C.; Stephan, D.W. Cationic aluminum hydride complexes: Reactions of carbene–alane adducts with trityl-borate. *Chem. Commun.* **2016**, *52*, 5305–5307. [CrossRef]
31. Baker, R.J.; Davies, A.J.; Jones, C.; Kloth, M. Structural and spectroscopic studies of carbene and N-donor ligand complexes of group 13 hydrides and halides. *J. Orgmet. Chem.* **2002**, *656*, 203–210. [CrossRef]
32. Gómez-Suárez, A.; Nelson, D.J.; Nolan, S.P. Quantifying and understanding the steric properties of N-heterocyclic carbenes. *Chem. Commun.* **2017**, *53*, 2650–2660. [CrossRef]
33. Poater, A.; Cosenza, B.; Correa, A.; Giudice, S.; Ragone, F.; Scarano, V.; Cavallo, L. SambVca: A web application for the calculation of the buried volume of N-heterocyclic carbene ligands. *Eur. J. Inorg. Chem.* **2009**, *2009*, 1759–1766. [CrossRef]
34. Vanden Broeck, S.M.; Nahra, F.; Cazin, C.S. Bulky-yet-flexible carbene ligands and their use in palladium cross-coupling. *Inorganics* **2019**, *7*, 78. [CrossRef]
35. Solovyev, A.; Ueng, S.-H.; Monot, J.; Fensterbank, L.; Malacria, M.; Lacôte, E.; Curran, D.P. Estimated Rate Constants for Hydrogen Abstraction from N-Heterocyclic Carbene−Borane Complexes by an Alkyl Radical. *Org. Lett.* **2010**, *12*, 2998–3001. [CrossRef]
36. Bantreil, X.; Nolan, S.P. Synthesis of N-heterocyclic carbene ligands and derived ruthenium olefin metathesis catalysts. *Nat. Protoc.* **2011**, *6*, 69–77. [CrossRef]
37. Mikhaylov, V.N.; Kazakov, I.V.; Parfeniuk, T.N.; Khoroshilova, O.V.; Scheer, M.; Timoshkin, A.Y.; Balova, I.A. The carbene transfer to strong Lewis acids: Copper is better than silver. *Dalton Trans.* **2021**, *50*, 2872–2879. [CrossRef]
38. Lavallo, V.; Canac, Y.; Präsang, C.; Donnadieu, B.; Bertrand, G. Stable cyclic (alkyl)(amino) carbenes as rigid or flexible, bulky, electron-rich ligands for transition-metal catalysts: A quaternary carbon atom makes the difference. *Angew. Int. Ed. Chem.* **2005**, *44*, 5705–5709. [CrossRef]
39. Berthon-Gelloz, G.; Siegler, M.A.; Spek, A.L.; Tinant, B.; Reek, J.N.; Markó, I.E. IPr* an easily accessible highly hindered N-heterocyclic carbene. *Dalton Trans.* **2010**, *39*, 1444–1446. [CrossRef]
40. Gómez-Suárez, A.; Ramón, R.S.; Songis, O.; Slawin, A.M.; Cazin, C.S.; Nolan, S.P. Influence of a very bulky N-heterocyclic carbene in gold-mediated catalysis. *Organometallics* **2011**, *30*, 5463–5470. [CrossRef]
41. *CrysAlisPro Software system*, version 1.171.39.46. Rigaku Oxford Diffraction. Rigaku Corporation: Oxford, UK, 2018.
42. Sheldrick, G.M. Crystal structure refinement with SHELXL. *Acta Cryst.* **2015**, *C71*, 3–8.
43. Farrugia, L.J. WinGX and ORTEP for Windows: An update. *J. Appl. Cryst.* **2012**, *45*, 849–854. [CrossRef]
44. Frisch, G.W.T.M.J.; Schlegel, H.B.; Scuseria, G.E.; Robb, M.A.; Cheeseman, J.R.; Scalmani, G.; Barone, V.; Petersson, G.A.; Nakatsuji, H.; Li, X.; et al. Gaussian 16 Revision A.03. Gaussian, Inc.: Wallingford, CT, USA, 2016.
45. Reed, A.E.; Curtiss, L.A.; Weinhold, F. Intermolecular interactions from a natural bond orbital, donor-acceptor viewpoint. *Chem. Rev.* **1988**, *88*, 899–926. [CrossRef]
46. Glendening, E.D.; Landis, C.R.; Weinhold, F. NBO 6.0: Natural bond orbital analysis program. *J. Comput. Chem.* **2013**, *34*, 1363–1374. [CrossRef] [PubMed]
47. Frisch, G.W.T.M.J.; Schlegel, H.B.; Scuseria, G.E.; Robb, M.A.; Cheeseman, J.R.; Scalmani, G.; Barone, V.; Mennucci, B.; Petersson, G.A.; Nakatsuji, H.; et al. Gaussian 09 Revision D.01. Gaussian, Inc.: Wallingford, CT, USA, 2013.

48. Zhao, Y.; Truhlar, D. The M06 suite of density functionals for main group thermochemistry, thermochemical kinetics, noncovalent interactions, excited states, and transition elements: Two new functionals and systematic testing of four M06-class functionals and 12 other functionals. *Theor. Chem. Acc.* **2008**, *120*, 215–241.
49. Jmol, An Open-Source JAVA Viewer for Chemical Structures in 3D. Available online: http://www.jmol.org (accessed on 4 December 2022).